Chemistry & Biology, Vol. 11, 319–326, March, 2004, ©2004 Elsevier Science Ltd. All rights reserved. DOI 10.1016/j.chembiol.2004.02.019

Crosslinking of and Coupling to Viral Capsid Proteins by Tyrosine Oxidation

Stéphane Meunier, Erica Strable, and M.G. Finn*
Department of Chemistry and
The Skaggs Institute for Chemical Biology
The Scripps Research Institute
10550 N. Torrey Pines Road
La Jolla, California 92037

Summary

Cowpea mosaic virus is composed of 60 identical copies of a two-subunit protein organized in pentameric assemblies around the icosahedral 5-fold symmetry axis. Treatment of the virus with the Ni(II) complex of the tripeptide GGH and a peroxide oxidant, or irradiation in the presence of $Ru(bpy)_3^{2+}$ and persulfate generates covalent crosslinks across the pentameric subunit boundaries, effectively stitching the subunits together. Intersubunit crosslinking was found to occur exclusively at adjacent tyrosine residues (Y52-Y103), as predicted from the X-ray crystal structure of the capsid, and to be more extensive with the photochemical ruthenium system. The Ni/GGH oxidative procedure was also used to make covalent attachments to the virion by trapping with a functionalized disulfide reagent.

Introduction

Cowpea mosaic virus (CPMV) is an icosahedral plant virus composed of 60 identical copies of a protein asymmetric unit assembled around a single-stranded RNA genome [1, 2]. Because of its high expression yields in its host plant, ease of isolation, stability, and known X-ray crystal structure [3], we have used it as a prototypical reagent to explore the limits of virus-based chemical reactions. At approximately 30 nm in diameter, the particles may be regarded as topologically analogous to dendrimers, but much larger in size and easier to prepare. Each protein asymmetric unit consists of two subunits, small (23 kDa, comprising the A domain) and large (41 kDa, B + C domains). The particle can also be described as the association of 12 pentamers of this asymmetric unit (Figure 1). CPMV chimeras can be readily prepared by site-directed mutagenesis or insertion of foreign sequences at precise sites on the viral capsid [4].

The chemical reactivity of CPMV is well defined and consistent with expectations based on its X-ray crystal structure. Thus, exposed lysine side chains may be addressed with activated ester electrophiles [5, 6], while the dearth of cysteines on the exterior surface of the capsid makes the particle poorly reactive with thiol-specific reagents [7]. Chimeras with one or more cysteines inserted at precise locations on each asymmetric unit have been created and are highly reactive toward maleimides and bromoacetamides, which permits the installation of functional molecules at well-defined locations [7–9]. CPMV particles are remarkably stable: they maintain their integrity for several days at room temperature at pH values from 3 to 9.5, and for many days in the presence of 20% of DMSO or DMF.

The present study concerns the effects of one-electron oxidation chemistry on the CPMV capsid. We focus here on the use of tripeptide NH_2-Gly-Gly-His-COOH (GGH) in the presence of nickel acetate [$Ni(OAc)_2$] and magnesium monoperoxyphthalate (MMPP), which was discovered by Kodadek and coworkers to mediate the efficient crosslinking of associated proteins in solution [10–12]. The peptide provides a favorable coordination environment for the nickel center, and a putative Ni(III) intermediate is thought to abstract an electron from the aromatic ring of an accessible tyrosine, leading to a tyrosyl radical after the loss of a proton (see Figure 3B). The highly activated radical intermediate couples either to a nearby tyrosine or nucleophilic side chain, such as a lysine or a cysteine, leading to a crosslinked adduct. This chemistry has been employed to determine the location of intermolecular contacts in multiprotein complexes [10, 13, 14], but viruses, the quintessential polyprotein assemblies, have not been so explored. We describe here the application of tyrosine oxidation chemistry to CPMV, resulting in specific subunit crosslinking.

Results and Discussion

Oxidation by Ni/GGH/MMPP

CPMV is indefinitely stable to the peracid MMPP and several other water-soluble two-electron and oxygen-atom-transfer oxidants. To a solution of CPMV (1 mg/ml) in phosphate buffer (pH 7.0) was added Ni/GGH/MMPP (in 1/1/1 ratio) at a stoichiometry of 10, 100, or 1000 equivalents of nickel per viral asymmetric unit. After incubation and quenching with an excess of β-mercaptoethanol, the samples were analyzed by denaturing gel electrophoresis, as shown in Figure 2A. The characteristic two bands of CPMV, corresponding to the large and small subunits, appear in lane 2. Lanes 3–7 show the results with increasing Ni/GGH/MMPP concentration. Notable is the appearance of higher molecular weight products in lanes 3–6, accompanied by a loss of intensity of the underivatized small subunit, with the large subunit band remaining unchanged. The new bands are found at positions corresponding to the expected molecular weights of dimers (46 kDa), trimers (69 kDa), tetramers (92 kDa), and pentamers (115 kDa) of the small subunit. While the pentamer appears to be formed in the greatest amount, no higher oligomers are observed. As discussed below, a separate band for the cyclic, rather than linear, pentamer would be expected, but is not observed with the nickel system. Examination of the putative linear pentamer by in-gel protease digestion and mass spectrometry identified it conclusively as deriving from the CPMV small subunit (data not shown).

*Correspondence: mgfinn@scripps.edu

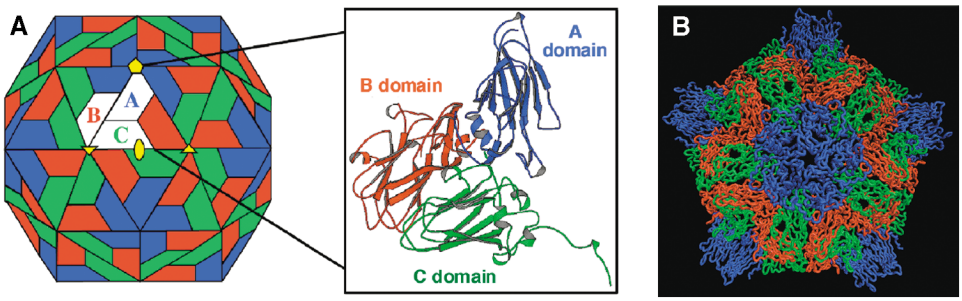

Figure 1. CPMV Structure

(A) Shown on the left is the subunit organization of CPMV; green and red represent the two domains of the large subunit, and blue represents the small subunit clustered around the 5-fold symmetry axes. On the right are the folds of the two subunits.

(B) View of 15 asymmetric units with the same color coding as in (A); note the organization of the small subunits about the 5-fold axis.

These observations are consistent with the formation of oxidative crosslinks between the small subunits around the 5-fold symmetry axis of the CPMV capsid. Omission of any of the three reagents [$Ni^{II}(OAc)_2$, GGH, or MMPP] completely prevents the formation of crosslinked material. The integrity of the crosslinked virus particles was verified by size-exclusion FPLC, sucrose gradient, and transmission electronic microscopy, all of which show particles with characteristics indistinguishable from the native particle (data not shown).

The best yield of crosslinked products was achieved using a moderate excess (100-fold) of Ni^{II}/GGH-MMPP per protein asymmetric unit (Figure 2A, lane 4); the use of 5000 equivalents of Ni/GGH/MMPP completely inhibited crosslinking (lane 7). The efficiency of the crosslinking process therefore appears to be a balance between the concentration of Ni(III) centers and a competitive quenching of tyrosyl radicals by excess reagent in solution; a reaction between oxidized tyrosine and the tripeptide GGH has been described [14]. Figure 2B shows that the reaction is largely complete within 1 min of mixing. No change was observed in the outcome after 19 hr at room temperature (data not shown). When a sample of oxidized CPMV was isolated after the optimized reaction conditions and resubjected to fresh reagents, no further crosslinking was observed.

Crosslinked CPMV was found to retain the lysine-based chemical reactivity of the untreated particle. Wild-type CPMV and the purified virus obtained from optimized Ni/GGH/MMPP treatment were treated with fluorescein-NHS ester under identical conditions. Quantitative measurement of the dye absorbance of the resulting particles established a loading of 68 $\pm$ 5 dyes/virion for CPMV and 59 $\pm$ 5 dyes/virion for the oxidized virus. Ultraviolet illumination of the SDS PAGE gels of these samples showed that both large and small subunit bands of CPMV were derivatized, as previously described [5]. The Ni/GGH/MMPP-treated virus similarly reacted at both unmodified subunits, but the degree of labeling of the crosslinked bands was inversely proportional to the size of the band (data not shown). Thus, while reactivity toward NHS esters is retained upon crosslinking, there may be one or more lysine sites that are at least partially blocked by oxidative treatment.

Inhibition and Trapping

The Ni/GGH/MMPP crosslinking reaction was inhibited by added tyrosine or tryptophan in a dose-dependent manner (complete inhibition with 50 equiv. of amino acid per virus asymmetric unit; data not shown), whereas serine had no effect up to 1000 equiv. Figure 3A shows the effect of cysteine and cystine on the process. The former was a good inhibitor of crosslinking at 1 mM (approximately 100 equivalents per asymmetric unit; Figure 3A, lanes 3–6), probably quenching the high-valent nickel species by virtue of its coordinating ability and reducing power. More interestingly, cystine, which is both a poorer ligand for metals and cannot be easily oxidized, also retarded oxidative crosslinking, albeit at higher concentration, showing dramatic but not quite complete inhibition at up to 10 mM (Figure 3A, lanes 7–10). While one cannot rule out the presence of low concentrations of cysteine in the cystine reactions (and vice versa), we suggest that cystine quenches intermedi-

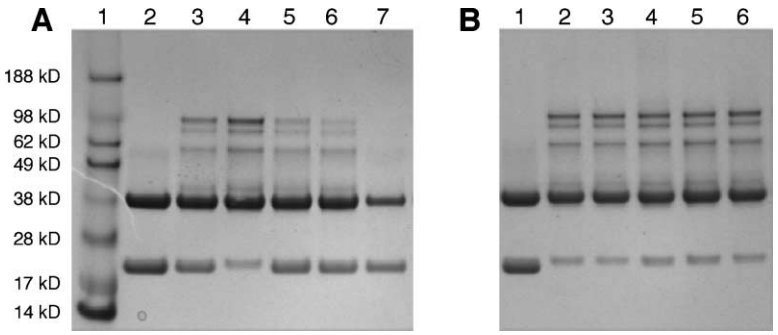

Figure 2. Crosslinking of CPMV Small Subunits

(A) SDS-PAGE gel showing wild-type CPMV (lane 2) and crosslinking reactions using 50, 100, 500, 1000, or 5000 equivalents of Ni/GGH/MMPP per viral asymmetric unit, respectively (lanes 3–7).

(B) Time course: lane 1, wild-type CPMV; lanes 2–6, crosslinking reaction using 100 equivalents of Ni/GGH/MMPP per asymmetric unit, quenched at 1, 3, 5, 7, and 10 min, respectively.

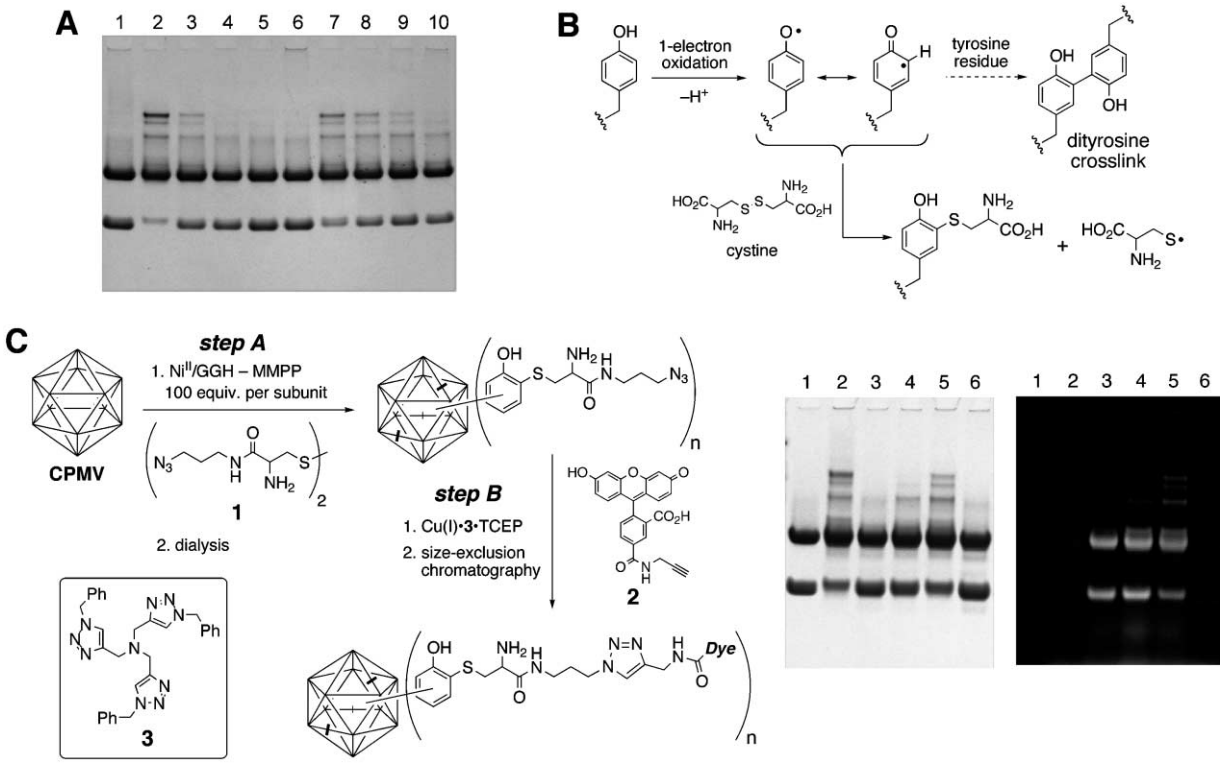

Figure 3. Inhibition of the Crosslinking Reaction by Cysteine and Cystine and Functionalization of CPMV

(A) Lane 1, CPMV; lane 2, control crosslinking reaction (100 equiv. Ni/GGH/MMPP per asymmetric unit); lanes 3–6, reactions in the presence of 0.5 mM, 1 mM, 5 mM, and 10 mM of cysteine; lanes 7–10, reactions in the presence of 0.5 mM, 1 mM, 5 mM, and 10 mM of cystine.

(B) Proposed mechanism for crosslinking and inhibition by cystine.

(C) Inhibition of crosslinking reaction by **1** and detection of the derivatized sites by Cu^{I}-catalyzed azide-alkyne cycloaddition. Lane 1, CPMV; lane 2, step A performed in the absence of **1**; lanes 3–5, step A performed in the presence of 5 mM, 3 mM, and 1 mM of **1**, respectively; lane 6, CPMV mixed with **1** in the absence of oxidant. Samples for all lanes were then subjected to step B with 2 mM $CuSO_4$, 5 mM **2**, 4 mM tris(carboxyethyl)phosphine, and 4 mM **3**. On the right (dark background) is shown the gel under ultraviolet illumination before Coumassie blue staining.

ate tyrosyl radicals on CPMV by disulfide cleavage and creation of a carbon-sulfur bond (Figure 3B).

These results suggested that it might be possible to functionalize tyrosine side chains on CPMV with a disulfide compound in the presence of Ni/GGH/MMPP. To this end, the azidoalkyl cystine derivative **1** was prepared and found to effectively inhibit crosslinking (Figure 3C), perhaps even better than cystine itself (Figure 3C, lane 2 versus lane 4). The formation of a covalent bond between CPMV and **1** in this process was assayed by coupling the fluorescein alkyne **2** to the azide using the aqueous-phase Cu^{I}-catalyzed azide-alkyne cycloaddition reaction recently developed by Fokin and Sharpless [15] and used in a growing list of bioconjugative applications [16–20]. Figure 3C shows that dye was attached to viral protein only after oxidative treatment in the presence of **1** (lanes 3–5). Both uncrosslinked and multimeric bands show dye labeling, demonstrating that tyrosine oxidation and capture occur at positions other than those responsible for crosslinking. The numbers of fluorescein molecules covalently attached to CPMV by this two-step process were roughly constant for a range of concentrations of **1**: 5 mM, 20 ± 5 dyes/particle; 3 mM, 26 ± 5 dyes/particle; 2 mM, 29 ± 5 dyes/particle; 1 mM, 20 ± 5 dyes/particle; and 0.5 mM, 32 ± 5 dyes/particle. While one might expect greater inhibition of crosslinking to correlate with greater numbers of attached inhibitor, not all labeled sites would be expected to be similarly reactive to the dye alkyne and copper catalyst.

Tyrosine-Knockout Mutations

The small subunit of CPMV contains five tyrosines at positions 11, 52, 93, 103, and 145 (Figure 4). Examination of the X-ray crystal structure of CPMV shows only one pair of residues, 52 and 103, to have phenolic rings adjacent to one another across a subunit interface, with the closest distance between aromatic carbons being 3.8 Å (Figure 4D). (The apparent close approach of residues 11 and 93 is an artifact of the perspective of this image; the aromatic rings of these two side chains are separated by 12.3 Å.) To determine the position(s) of crosslinking, Phe-for-Tyr mutants (chimeras) were prepared by site-directed mutagenesis [2, 21], with the results shown in Figure 5. Y145F, Y93F, and Y11F mutants were crosslinked in a manner indistinguishable from wild-type upon treatment with Ni/GGH/MMPP, including the response to variations in the concentration of the oxidative reagent. In contrast, the Y52F and Y103F mutants were found to be completely resistant to crosslink-

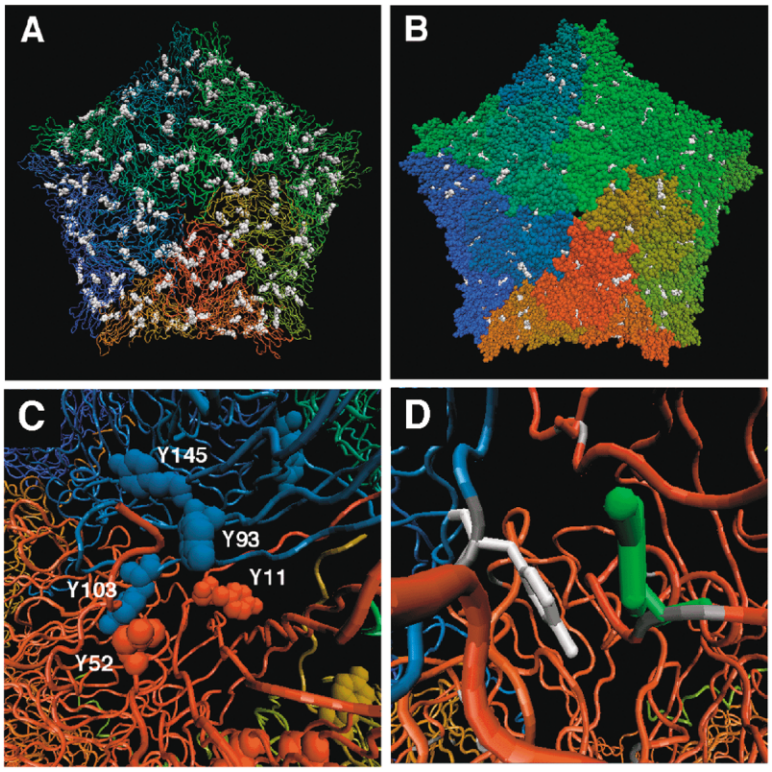

Figure 4. Views of theX-Rray Crystal Structure of CPMV

(A) The exterior surface of the pentamer (the asymmetric units around the 5-fold symmetry axis), with tyrosine residues in white and the carbon backbone of the asymmetric units in different colors.

(B) Tyrosines are shown in white; asymmetric units are shown in CPK representation to reveal surface-exposed residues.

(C) Expanded image of the boundary between blue and red small subunits, showing the protein backbone except for tyrosines in CPK representation.

(D) Expanded image showing the close contact between Y52 (green) and Y103 (white) of adjacent subunits. 3.81 Å separates the *ipso* carbon (*para* to OH) of Y52 and one of the carbons *ortho* to OH of Y103. These images were created with the VMD program [22] using oligomer coordinates generated by the VIPER website [23] derived from the X-ray crystal structure (Protein database ID code 1NY7).

ing over the entire range of oxidant concentrations examined.

Oxidative crosslinking was accompanied by the appearance of a fluorescence emission band at approximately 400 nm (Figure 6), consistent with the production of dityrosine units. Control experiments omitting either Ni/GGH or MMPP gave no such band (Figure 6A). This well-defined emission may be assigned to the 52-103 dityrosine crosslink on the basis of observations with the F-for-Y mutants (Figure 6B). The three chimeras that gave crosslinked multimers in SDS-PAGE also showed a prominent fluorescence emission band after oxidation, at slightly longer wavelength than wild-type. In contrast, the noncrosslinking Y52F and Y103F particles gave enhanced emission in the 370–500 nm range but not a clearly defined peak. These data are consistent with the formation of conjugated crosslinks (probably involving other residues as well as tyrosine) at other positions, along with selective inter-subunit dityrosine linkages between Y52 and Y103.

Ruthenium-Mediated Photochemical Crosslinking

Visible-light irradiation in the presence of ruthenium(II) tris(bipyridyl) dication [$Ru(bpy)_3^{2+}$] and an electron acceptor such as ammonium persulfate (APS) induces very efficient crosslinking between contacting proteins; because of its speed, this system is also highly useful for the covalent capturing of protein-protein interactions [24–26]. The mechanism has been assumed to be similar to that of Ni/GGH/MMPP, and one report of the formation

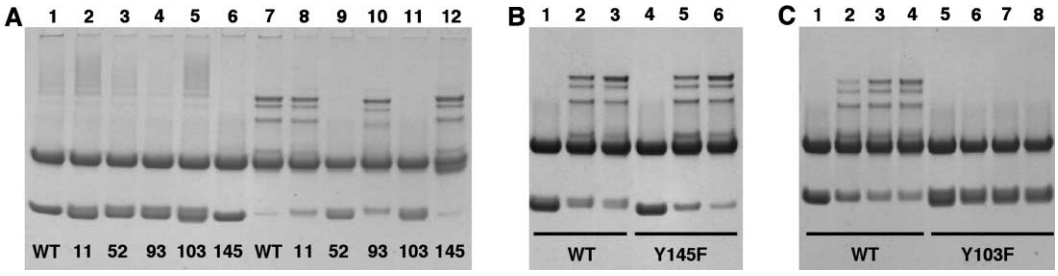

Figure 5. Reactivity of Y-to-F Mutants

(A) Lanes 1–6, before oxidative treatment; lanes 7–12, after oxidative treatment (100 equiv. Ni/GGH/MMPP per asymmetric unit). The position of the Y-to-F replacement is given at the bottom of each lane.

(B and C) Response to changes in Ni/GGH/MMPP concentration for two representative cases in comparison to wild-type. (B), lanes 1–3, CPMV with 0, 50, and 100 equiv. of Ni/GGH/MMPP per asymmetric unit, respectively; lanes 4–6, Y145P under the same set of conditions. (C), lanes 1–4, CPMV with 0, 50, 100, and 500 equiv. of Ni/GGH/MMPP per asymmetric unit, respectively; lanes 5–8, Y103F under the same set of conditions.

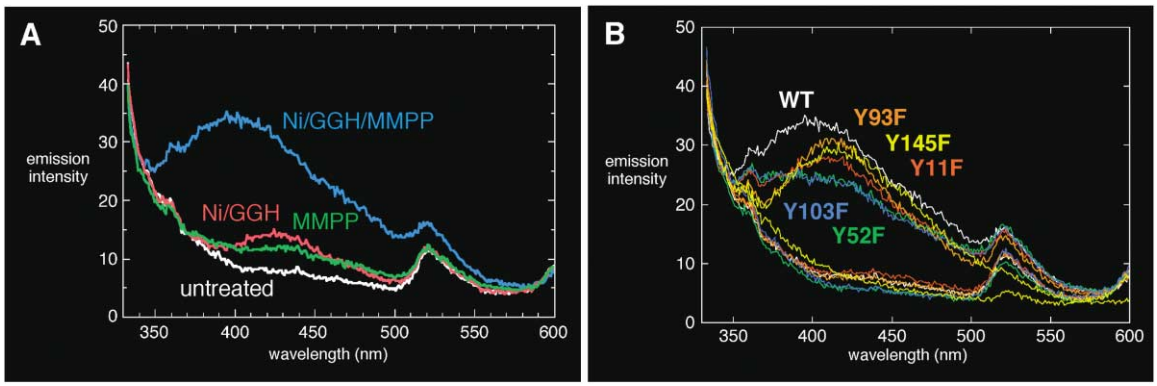

Figure 6. Fluorescence Detection of Dityrosine Crosslinks

(A) Emission spectra (excitation at 323 nm) of wild-type CPMV (white), CPMV treated with 100 equiv. Ni/GGH/MMPP per asymmetric unit (blue), CPMV treated with Ni/GGH (omitting MMPP, red), and CPMV treated with MMPP alone (green), all containing virus at 1mg/ml.

(B) Emission spectra of wild-type and mutant CPMV before (unlabeled spectra) and after (labeled spectra) treatment with Ni/GGH/MMPP (100 equiv. per asymmetric unit). All samples contained virus at 1.0 mg/ml.

of dityrosine linkages has appeared [27]. Figure 7A shows the results of a preliminary assessment of $Ru(bpy)_3^{2+}$-mediated photochemical crosslinking. A comparison of lanes 1 and 3 shows that all of the bands observed with Ni/GGH/MMPP were also found with the photochemical method, with the same concomitant decrease in the intensity of the band due to the unmodified small, but not the large, subunit. An additional strong band appears above the highest molecular weight band for the Ni/GGH/MMPP reaction. Mass spectrometry data following in-gel protease digestion of this material was nearly identical to that of the linear pentamer (data not shown). We therefore assign this band to the cyclic pentamer created by constructing all five possible crosslinks between small subunits. Its diminished mobility on electrophoresis compared with the linear pentamer (which is made by four subunit crosslinks) mirrors the relative positions of linked versus linear pentamers in the "chain mail" capsid of mature bacteriophage HK97 [28]. Figure 7B shows the expected inhibition of photochemical crosslinking with increasing concentrations of added histidine, which is capable of intercepting the putative Ru(III) oxidative species. Note that this competition eliminated the highest molecular weight bands first as histidine concentration was raised, as expected for the inhibition of a sequential stepwise process.

The Phe-for-Tyr mutants behaved similarly in the photoactivated reaction as in the Ni/GGH/MMPP process: Y52F and Y103 were resistant to crosslinking, whereas the behavior of Y11F, Y93F, and Y145F was indistinguishable from wild-type. It is therefore very likely that the crosslinking mechanisms of the Ni/GGH/MMPP and $Ru(bpy)_3^{2+}$/APS systems are similar and involve the formation of dityrosine units. The latter reagent is more potent, as demonstrated by the formation of cyclic pentamers and the greater weighting of the product distribution toward the higher oligomers.

Particle Stability

Crosslinking of viral subunits may, in principle, make virions more resistant to disassembly; a spectacular example is provided by the natural chain mail architecture of bacteriophage HK97 [29]. Wild-type CPMV, before and after optimized Ni-GGH-MMPP crosslinking, was exposed to heat and extremes of pH and monitored by size-exclusion FPLC. No differences in stability were observed between native and crosslinked capsids. Both are stable for more than 2 days in the presence of 20% DMSO at room temperature and for more than 4 days over a range of pH from 3.0 to 9.5 at room temperature, but lose integrity after 15 min at 50°C.

We suggest that a positive effect on the stability of the 60-unit assembly can be achieved only when the protein interface being crosslinked is important to particle integrity and when a high percentage of such connections are made. Neither condition appears to be sat-

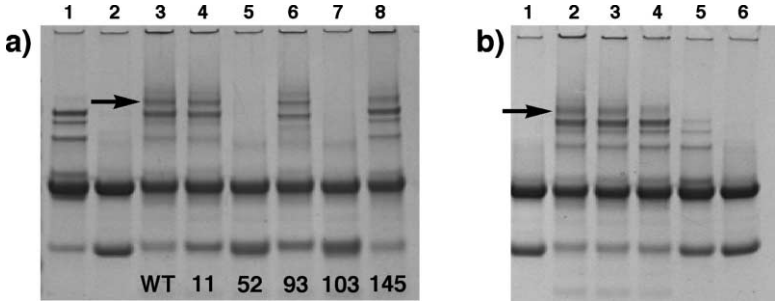

Figure 7. Reactivity of CMPV under Oxidative Photochemical Conditions

The arrows mark the position of the cyclic pentamer band in each gel.

(A) Lane 1, CMPV oxidized by 100 equiv. Ni/GGH/MMPP; lane 2, wild-type CPMV; lanes 3–8, CMPV and Phe-for-Tyr mutants treated with 12.5 equiv. $[Ru(bpy_3^{2+}]Cl_2$ + 250 equiv. APS and photolyzed using a 150-W Xe arc lamp for 1 s.

(B) Lane 1, wild-type CPMV; lanes 2–6, CMPV photooxidized as in (A) in the presence of 0, 1, 10, 100, and 1000 equiv. of histidine per protein asymmetric unit, respectively.

isfied in this case, as follows. The small subunit pentameric interface being crosslinked by the observed dityrosine is already the strongest interface in CPMV, as evaluated by buried surface area association energies [23, 30]. By this criterion, the interface between the small and large subunits is the "weakest link" of the assembled particle and so is predicted to be the site at which crosslinking has the best chance to improve particle stability. Furthermore, since pure CPMV protein cannot be induced to self-assemble around its own genome outside of the host cell, CPMV particle stability is likely to be a kinetic, rather than a thermodynamic, phenomenon. Capsid decomposition (separation of asymmetric units from each other, which may or may not be concomitant with denaturation of subunit conformations) should be irreversible after a certain point. Recent work showing a high degree of cooperativity in subunit association only at the very late stages of capsid assembly for a different virion [31, 32] suggests that such an irreversible stage will come early in the decomposition process. It is therefore likely that stabilization of capsids by subunit crosslinking will require complete (or nearly complete) stitching of the most crucial subunit interfaces, which represents a goal of studies currently in progress.

Significance

The use of the Ni/GGH/MMPP reagent has been shown to both induce crosslinking between tyrosine residues in adjacent subunits of the CPMV structure and to generate tyrosyl radicals at other positions which are amenable to trapping with external disulfide reagents. The generation of a specific crosslink between Y52 and Y103 is a consequence of the close proximity of their aromatic rings in roughly coplanar alignment. Tyrosine 52 is accessible to solvent on the exterior surface of the particle, and so it is likely that this residue is oxidized first, and then coupling to Y103 occurs. Many, but not all, of the small subunits are crosslinked in this fashion, and extended or repeated treatment with the oxidizing reagent fails to give increasing amounts of such crosslinking. This suggests that trapping of the tyrosyl radical of Y52 by a different protein residue (or an external species) is somewhat competitive with crosslinking at Y103. Y93 is similarly accessible to solvent, but its oxidized tyrosine apparently cannot reach Y11 before undergoing an alternative (noncrosslinking) trapping or quenching event. The $Ru(bpy)_3^{2+}$/APS photochemical system operates by a similar mechanism and gives more complete crosslinking reactivity. The choice of oxidant depends on the user's need for convenience (Ni/GGH) versus high reactivity (Ru photochemistry).

From a practical standpoint, the use of functionalized disulfides, as demonstrated here with azide reagent 1 and its subsequent derivatization with alkyne 2, comprises a means to address the virus particle that is independent of standard coupling methods such as lysine acylation, carboxylate amidation, and thiol alkylation. Most interestingly, these results suggest that it may be possible to stitch virus particles together at different subunit boundaries by designed positioning of tyrosine residues in order to achieve more stable structures. Nature's use of covalent crosslinks to make an extraordinarily thin and tough capsid in bacteriophage HK97 is both an inspiration and a challenge to protein engineering on a nanochemical scale [29].

Experimental Procedures

Propagation and Purification of CMPV

CPMV was propagated in black-eyed peas and isolated according to a standard protocol [33]; 40 g of leaf tissue was typically used, wild-type and mutants each providing approximately 40 mg of virus. Purification was accomplished by ultracentrifugation (2 hr, 38,000 rpm, Beckman-Coulter SW41 rotor, 4°C) through a sucrose gradient prepared with 10% and 30% sucrose solutions on a Biocomp Gradient Master instrument. Purified viruses were analyzed by size exclusion chromatography (Superose 6 column); wild-type CMPV and the Tyr-for-Phe mutants shared a retention volume of 11 ml (0.4 ml/min flow rate). Dialyses were performed with 10,000 molecular weight cut-off tubing.

Site-directed mutagenesis of the cDNA encoding for the coat protein of CPMV was carried out as previously described [8]. The primers used for the mutagenesis were as follows: Y11F, F 5′-CT GAA GCC TCA GAT GTG TTC AGC CCA TGT ATG ATA G–3′, R 5′-CTATCATACATGGGCTGAACACATCTGAGGCTTCAG-3′; Y52F, F 5′-GGAATACGCACATTTTCAATCCTCCAATTATGAATGTG-3′, R 5′-CACATTCATAATTGGAGGATTGAAAATGTGCGTATTCC-3′; Y93F, F 5′-GGTCAAGTCTTTGTTTTCCTGCGCCAGTCCATGAACC-3′, R 5′-GGTTCATGGACTGGCGCAGGAAAACAAAGACTTGACC-3′; Y103F; F 5′-AACCCTGAAAGTTTTGATGCGCGGACA-3′, R 5′-TGTCCGGCG ATCAAAACTTTCAGGGTT-3′; Y145F; F 5′-CAGACCACCTGGTTCC TTGAATGTGTTGCT-3′, R 5′-AGCAACACATTCAAGGAACCAGGT GGTGTC-3′.

Crosslinking Reactions

Standard nickel-mediated crosslinking reactions were performed in a total volume of 100 μl, with the following final concentrations: 0.1 M potassium phosphate buffer (pH 7.0), 1.0 mg/ml CPMV (10.7 μM in protein asymmetric unit), and 1.0 mM Ni(II)/GGH. The nickel complex was prepared as an equimolar (100 mM each) mixture of $Ni(OAc)_2$ and Gly-Gly-His in water; both reagents were obtained from Aldrich. The reactions were initiated by the addition of MMPP (Aldrich) to a concentration of 1.0 mM, incubated at room temperature for 30 min unless otherwise noted, and quenched by the addition of 4 μl of 4 M β-mercaptoethanol. Samples to be used in subsequent dye attachment reactions were instead quenched by extensive dialysis in 0.1 M phosphate buffer.

Photochemical crosslinking reactions were performed in a total volume of 50 μl, with the following final concentrations: 0.1 M potassium phosphate buffer (pH 7.0), 1.0 mg/ml CPMV, 0.125 mM tris(2,2′-bipyridyl)ruthenium(II)chloride hexahydrate (Aldrich), and 2.5 mM ammonium persulfate (Aldrich). The last two reagents were added immediately prior to irradiation, which was performed for 1 s using a 150-W Xe arc lamp (ICL Technologies, intensity 15 A). The light was filtered through 10 cm of distilled water, and the tube was placed parallel to the light source at a distance of 50 cm. Immediately after irradiation, the reactions were quenched by the addition of 2 μl of 4 M β-mercaptoethanol and analyzed by denaturing gel electrophoresis.

Dye Attachments via Disulfide Reagent 1

Crosslinking reactions in the presence of **1** were performed with the above protocol, with **1** added to the mixture just prior to addition of oxidant. Following overnight dialysis of the reaction mixture in phosphate buffer, the virus solutions were concentrated to approximately 2.3 mg/ml (using Amicon Ultra 100,000 molecular weight cut-off filters, Millipore). The Cu^{I}-catalyzed azide-alkyne cycloaddition reactions were then carried out according to the previously optimized protocol [16].

Synthesis of Reagent 1

To a solution of $(Boc\text{-}Cys\text{-}OH)_2$ (Bachem, 2.00 g, 4.54 mmol) in THF (100 ml) was added N-hydroxysuccinimide (1.15 g, 9.10 mmol) and

dicyclohexylcarbodiimide (2.06 g, 9.10 mmol) at 0°C. The solution was stirred for 16 hr at room temperature, filtered, and evaporated under reduced pressure to afford 2.28 g (79%) of (Boc-Cys-OSu)$_2$ ($C_{24}H_{34}N_4O_{12}S_2$, 634.69 g/mol), which was used without further purification. ^{1}H NMR ($CDCl_3$, δ) 1.45 (s, 9H, $O(CH_3)_3$); 2.80 (s, 4H, $C(O)CH_2CH_2C(O)$); 3.32 (td, J = 15.0, 10.0 Hz, 2H, CH_2S); 4.90–5.05 (m, 1H, CHC(O)), 5.42–5.60 (m, 1H, NHC(O)).

To a solution of (Boc-Cys-OSu)$_2$ (1.42 g, 2.24 mmol) in THF (50 ml) was added 3-azidopropylamine (5.33 ml of a 0.92 M solution in toluene, 4.90 mmol). (This reagent was prepared from 3-chloropropylamine hydrochloride by reaction with NaN_3 in water at 90°C, followed by adjustment to pH 11 and extraction into toluene. Caution: do not remove all of the solvent, as the pure compound is potentially explosive.) The reaction was stirred at room temperature for 16 hr and then evaporated under reduced pressure. The residue was purified by column chromatography (CH_2Cl_2/MeOH 98/2) to afford 640 mg (47%) of (Boc-Cys-3-azidopropyl)$_2$ ($C_{22}H_{40}N_{10}O_6S_2$, 604.76 g/mol). TLC (CH_2Cl_2/MeOH 98/2): R_f = 0.26. ^{1}H NMR ($CDCl_3$, δ) 1.42 (s, 9H, $O(CH_3)_3$; 1.80 (p, J = 8.7 Hz, 2H, $CH_2CH_2CH_2$); 2.80–3.05 (m, 2H, CH_2N_3); 3.20–3.50 (m, 4H, CH_2NH, CH_2S); 4.65–4.93 (m, 1H, CHC(O)); 5.55 (d, J = 12.5 Hz, 1H, NHC(O)); 7.75–7.95 (m, 1H, NHC(O)).

To the Boc-protected azide (640 mg, 1.06 mmol) in CH_2Cl_2 (30 ml) was added 3 ml trifluoroacetic acid. The solution was stirred at room temperature for 4 hr and evaporated under reduced pressure to afford 660 mg (quantitative yield) of **1** ($C_{12}H_{24}N_{10}O_2S_2.2CF_3COOH$, 632.52 g/mol). ^{1}H NMR (CD_3OD, δ) 1.75 (p, J = 9.0 Hz, 2H, $CH_2CH_2CH_2$); 3.05 (dd, J = 13.7, 7.5 Hz, 1H, CH_AH_BS); 3.10–3.55 (m, 5H, CH_AH_BS, CH_2NH, CH_2N_3); 8.10 (dd, J = 7.5, 6.2 Hz, 1H, CHC(O)). Electrospray mass spectrum, m/z: 405 ([M+H]$^+$); 427 ([M+Na]$^+$).

Analytical Methods

Samples for gel electrophoresis (12 μl of solutions containing ~1 mg/ml virus) were mixed with 5 μl of 4× loading buffer (NuPage LDS sample buffer, Invitrogen) and 3 μl of 1 M DTT, heated at 95°C for 5 min, and then analyzed at 100 V on 10% NuPAGE Bis-Tris gels (Invitrogen). Bands were visualized by staining with Simply Blue SafeStain (Invitrogen). For dye attachment experiments, the protein bands were visualized under ultraviolet illumination before staining. Fluorescence spectra (excitation at 323 nm) were recorded with a Cary Eclipse spectrophotometer (Varian, Inc.) on virus solutions of 1.0 mg/ml in 0.1 M phosphate buffer (pH 7.0). Procedures and data for in-gel digestion and MALDI-MS of linear and cyclic pentamer bands are omitted for length and are available from the authors upon request.

Acknowledgments

We thank the David and Lucille Packard Foundation, the National Institutes of Health, The Skaggs Institute of Chemical Biology, the La Jolla Interfaces in Science Program, the Burroughs Wellcome Fund (E.S. is an LJIS fellow), and the Association pour la Recherche sur le Cancer for support of this work. We are grateful to Dr. Qian Wang and Profs. Thomas Kodadek and Vijay Reddy for valuable discussions and to Dr. Wang and Ms. Elaine Yang for the Y145F mutant.

Received: October 2, 2003
Revised: December 5, 2003
Accepted: December 8, 2003
Published: March 19, 2004

References

1. Johnson, J.E., and Speir, J.A. (1997). Quasi-equivalent viruses: a paradigm for protein assemblies. J. Mol. Biol. *269*, 665–675.
2. Dessens, J.T., and Lomonossoff, G.P. (1993). Cauliflower mosaic virus 35S promoter-controlled DNA copies of cowpea mosaic virus RNAs are infectious on plants. J. Gen. Virol. *74*, 889–892.
3. Lin, T., Chen, Z., Usha, R., Stauffacher, C.V., Dai, J.-B., Schmidt, T., and Johnson, J.E. (1999). The refined crystal structure of cowpea mosaic virus at 2.8 Å resolution. Virology *265*, 20–34.
4. Johnson, J., Lin, T., and Lomonossoff, G. (1997). Presentation of heterolgous peptides on plant viruses. Annu. Rev. Phytopathol. *35*, 67–86.
5. Wang, Q., Kaltgrad, E., Lin, T., Johnson, J.E., and Finn, M.G. (2002). Natural supramolecular building blocks: wild-type cowpea mosaic virus. Chem. Biol. *9*, 805–811.
6. Raja, K.S., Wang, Q., Gonzalez, M.J., Manchester, M., Johnson, J.E., and Finn, M.G. (2003). Hybrid virus-polymer materials. 1. Synthesis and properties of PEG-decorated cowpea mosaic virus. Biomacromolecules *4*, 472–476.
7. Wang, Q., Lin, T., Tang, L., Johnson, J.E., and Finn, M.G. (2002). Icosahedral virus particles as addressable nanoscale building blocks. Angew. Chem. Int. Ed. Engl. *41*, 459–462.
8. Wang, Q., Lin, T., Johnson, J.E., and Finn, M.G. (2002). Natural supramolecular building blocks: cysteine-added mutants of cowpea mosaic virus. Chem. Biol. *9*, 813–819.
9. Wang, Q., Raja, K.S., Janda, K.D., Lin, T., and Finn, M.G. (2003). Blue fluorescent antibodies as reporters of steric accessibility in virus conjugates. Bioconjug. Chem. *14*, 38–43.
10. Brown, K.C., Yang, S.-H., and Kodadek, T. (1995). Highly specific oxidative crosslinking of proteins mediated by a nickel-peptide complex. Biochemistry *34*, 4733–4739.
11. Fancy, D.A., and Kodadek, T. (1998). A critical role for tyrosine residues in His6Ni-mediated protein crosslinking. Biochem. Biophys. Res. Commun. *247*, 420–426.
12. Amini, F., Kodadek, T., and Brown, K.C. (2002). Protein affinity labeling mediated by genetically encoded peptide tags. Angew. Chem. Int. Ed. Engl. *41*, 356–359.
13. Fancy, D.A., Melcher, K., Johnston, S.A., and Kodadek, T. (1996). New chemistry for the study of multiprotein complexes: the six-histidine tag as a receptor for a protein crosslinking reagent. Chem. Biol. *3*, 551–559.
14. Person, M.D., Brown, K.C., Mahrus, S., Craik, C.S., and Burlingame, A.L. (2001). Novel inter-protein cross-link identified in the GGH-ecotin D137Y dimer. Protein Sci. *10*, 1549–1562.
15. Rostovtsev, V.V., Green, L.G., Fokin, V.V., and Sharpless, K.B. (2002). A stepwise huisgen cycloaddition process: copper(I)-catalyzed regioselective ligation of azides and terminal alkynes. Angew. Chem. Int. Ed. Engl. *41*, 2596–2599.
16. Wang, Q., Chan, T.R., Hilgraf, R., Fokin, V.V., Sharpless, K.B., and Finn, M.G. (2003). Bioconjugation by copper(I)-catalyzed azide-alkyne [3+2] cycloaddition. J. Am. Chem. Soc. *125*, 3192–3193.
17. Speers, A.E., Adam, G.C., and Cravatt, B.F. (2003). Activity-based protein profiling *in vivo* using a copper(I)-catalyzed azide-alkyne cycloaddition. J. Am. Chem. Soc. *125*, 4686–4687.
18. Fazio, F., Bryan, M.C., Blixt, O., Paulson, J.C., and Wong, C.-H. (2002). Synthesis of sugar arrays in microtiter plates. J. Am. Chem. Soc. *124*, 14397–14402.
19. Seo, T.S., Li, Z., Ruparel, H., and Ju, J. (2003). Click chemistry to construct fluorescent oligonucleotides for DNA sequencing. J. Org. Chem. *68*, 609–612.
20. Deiters, A., Cropp, T.A., Mukherji, M., Chin, J.W., Anderson, J.C., and Schultz, P.G. (2003). Adding amino acids with novel reactivity to the genetic code of *Saccharomyces cerevisiae*. J. Am. Chem. Soc. *125*, 11782–11783.
21. Lin, T., Porta, C., Lomonossoff, G., and Johnson, J.E. (1996). Structure-based design of peptide presentation on a viral surface: the crystal structure of a plant/animal virus chimera at 2.8 Å resolution. Fold. Des. *1*, 179–187.
22. Humphrey, W., Dalke, A., and Schulten, K. (1996). VMD: visual molecular dynamics. J. Mol. Graph. *14*, 33–38.
23. Reddy, V., Natarajan, P., Okerberg, B., Li, K., Damodaran, K., Morton, R., Brooks, C.I., and Johnson, J. (2001). VIrus Particle ExploreR (VIPER), a website for virus capsid structures and their computational analyses. J. Virol. *75*, 11943–11947.
24. Fancy, D.A., and Kodadek, T. (1999). Chemistry for the analysis of protein-protein interactions: rapid and efficient cross-linking triggered by long wavelength light. Proc. Natl. Acad. Sci. USA *96*, 6020–6024.
25. Fancy, D.A., Denison, C., Kim, K., Xie, Y., Holdeman, T., Amini, F., and Kodadek, T. (2000). Scope, limitations and mechanistic aspects of the photo-induced cross-linking of proteins by water-soluble metal complexes. Chem. Biol. *7*, 697–708.

26. Xie, Y., Denison, C., Yang, S.-H., Fancy, D.A., and Kodadek, T. (2000). Biochemical characterization of the TATA-binding protein-Gal4 activation domain complex. J. Biol. Chem. *275*, 31914–31920.
27. Andreev, O.A., Reshetnyak, Y.K., and Goldfarb, R.H. (2002). Evidence of inter- and intra-molecular crosslinking of tyrosine residues of calmodulin induced by photo-activation of ruthenium(II). Photochem. Photobiol. Sci. *1*, 834–836.
28. Duda, R.L. (1998). Protein chainmail: catenated protein in viral capsids. Cell *94*, 55–60.
29. Wikoff, W.R., Liljas, L., Duda, R.L., Tsuruta, H., Hendrix, R.W., and Johnson, J.E. (2000). Topologically linked protein rings in the bacteriophage HK97 capsid. Science *289*, 2129–2133.
30. Eisenberg, D.S., and McLachlan, A.D. (1986). Solvation energy in protein folding and binding. Nature *319*, 199–203.
31. Ceres, P., and Zlotnick, A. (2002). Hepatitis B virus capsid assembly is driven by weak intersubunit contacts. Biochemistry *41*, 11525–11531.
32. Singh, S., and Zlotnick, A. (2003). Observed hysteresis of virus capsid disassembly is implicit in kinetic models of assembly. J. Biol. Chem. *278*, 18249–18255.
33. Wellink, J. (1998). Comovirus isolation and RNA extraction. In Plant Virology Protocols, G. Foster and S. Taylor, eds. (Totowa, NJ: Humana Press), p. 205.